Three-dimensional reduced-graphene oxide/Fe_3O_4/Hydroxypropyl-β-cyclodextrin nanocomposite enhanced electrochemical sensing for the simultaneous quantification of serotonin, dopamine and ascorbic acid

Wenting Liang[a*], Yanqin Rong[a], Lifang Fan[a], Caihong Zhang[a], Wenjuan Dong[a], Jing Li[a], Jianping Niu[b*], Cheng Yang[c*], Shaomin Shuang[a], Chuan Dong[a], Wai-Yeung Wong[d*]

[a] Institute of Environmental Science, Department of Chemistry, Shanxi University, Taiyuan 030006, China. Email: liangwt@sxu.edu.cn

[b] Department of Neurosurgery, Shanxi academy of Medical Sciences Shanxi Dayi Hospital, Taiyuan 030006, China. Email: niujianping0032@126.com

[c] College of Chemistry and Healthy Food, Evaluation Research Center, West China Medical School, Sichuan University, Chengdu 610064, China. E-mail: yangchengyc@scu.edu.cn

[d] Department of Applied Biology and Chemical Technology, The Hong Kong Polytechnic University, Hung Hom, Hong Kong 999077, China. E-mail: wai-yeung.wong@polyu.edu.hk

Abstract

In the present work, three-dimensional reduced graphene oxide containing Fe_3O_4 nanoparticles have been successfully decorated with hydroxypropyl-β-cyclodextrin (HP-β-CD) to construct a novel nanocomposite (3D-rGO/Fe_3O_4/HP-β-CD). The 3D-rGO/Fe_3O_4/HP-β-CD was further coated on a glassy carbon electrode (GCE) to design an electrochemical sensing platform for detecting simultaneously of serotonin (5-HT), dopamine (DA), and ascorbic acid (AA). The interconnected porous reduced graphene oxide framework tightly anchored to Fe_3O_4 magnetic nanoparticles warrants good electrical conductivity and efficient catalytic activity. The HP-β-CD acts as a supramolecular host with high recognition ability for 5-HT, DA and AA. Benefiting from the above charming peculiarity, well-separated oxidation peaks and increased peak currents were observed for 5-HT, DA, and AA individually and in mixtures by differential pulse voltammetry (DPV). The following figures of merit were found for simultaneous electrochemical determination of 5-HT, DA, and AA: (a) Well separated peaks at around 0.316, 0.16 and -0.044 V (vs. glassy

carbon electrode, GCE); (b) linear responses in the 0.01 - 25 μM, 0.02 - 25 μM and 10 - 350 μM; (c) detection limits of 3.3 nM, 6.7 nM and 3.3 μM (S/N = 3), and (d) recoveries of 96.9%-103%, 97.3%-102% and 96.3%-105% from spiked serum samples, respectively, and relative standard deviation (RSD) all less than 4% .

Keywords Three-dimensional reduced-graphene oxide; Magnetic nanoparticles; Hydroxypropyl-β-cyclodextrin; Electrochemical sensing platform; Simultaneous determination

1. Introduction

Serotonin (5-hydroxytryptamine, 5-HT) and ascorbic acid (AA) frequently coexist in biological fluids, which make the extremely vital contribution to maintaining the functions of human metabolism, central nervous and circulatory system [1, 2]. Dopamine (DA), known as an important neurotransmitter, widely exists in the brain for message transfer [3]. In general, low levels of DA can bring about neurological disorders including Parkinson's disease, schizophrenia and HIV infection [4, 5]. For the treatment of these illnesses, there is a demand to supply the appropriate amounts of DA to the patients and further to monitor the changes of DA in their serum regularly. However, 5-HT and AA are always co-present in serum, causing some interference for the detection of DA. Thus, it is of especial importance to develop a rapid and simple assay to determine concentration of DA in the presence of 5-HT and AA.

Currently, electrochemical methods show the bigger promise in the detection of small biomolecules compared to other strategies including fluorometric, chromatographic, spectrophotometric, chemiluminescent and so on [6]. Due to the minimally invasive, low-cost and rapid diagnoses for patients, it has been tried as the effective means for the analyses of active molecules in the biological systems [7-9]. Nevertheless, the biggest barrier for simultaneous electrochemical determination of 5-HT, DA and AA is the similar oxidation potentials of these three targets on general electrodes resulting in an overlapping oxidation peak. Unluckily, there only exist a few composite materials as the sensitive coating of electrodes or attached to electrodes by electrochemically pre-treated method, which have been explored to determine these three analytes simultaneously, such as polymers [10], acetylcholine [11] and carbon-spheres [12]. Consequently, the research interest has focused on exploiting suitable functionalized materials to further promote the sensitivity and selectivity of electrode for simultaneously detecting of these three biomolecules.

3D-graphene-based nanocomposites are considered to be a promising electrode material for electrochemical biosensor, thanking to their ultrahigh surface-area-to-volume ratio, improved electron transfer and mass transport [13-17]. Fe_3O_4, magnetic nanoparticles, possess considerable catalytic ability, together with great surface activity and favorable magnetic properties [18], it has been used to functionalize three-dimensional reduced graphene oxide (3D-rGO). By the preparation of Fe_3O_4 loaded 3D-rGO materials (3D-rGO/Fe_3O_4), it can enhance their existing merits synergistically [19-21]. Nevertheless, 3D-rGO/Fe_3O_4 composites suffer from the disadvantages of poor water solubility and lack of selectivity. This still hinders their great promise in electrochemical aspects, so it is highly desired to explore certain modifiers to improve their hydrophilicity, dispersion and recognizability. Interestingly, cyclodextrins (CDs) have commonly emerged as a functional water-soluble unit to improve the dispersibility and stability of graphene family nanomaterials and achieve remarkable electrochemical behavior by supramolecular selectivity [22, 23]. The CD-related host-guest interactions have potentially exerted a profound effect on the electrochemical sensing [24-26]. It has been demonstrated that CD and CD derivatives are highly efficient in specific molecular recognition and stereodifferentiation [27, 28], even revealing the inclusion interaction towards 5-HT [29], DA [30] and AA [30].

Herein, we develop an efficient strategy for the generation of HP-β-CD functionalized 3D-rGO/Fe_3O_4 (3D-rGO/Fe_3O_4/HP-β-CD) and explore its adhibition in the simultaneous electrochemical detection of 5-HT, DA and AA, as shown in scheme 1. The 3D-rGO/Fe_3O_4/HP-β-CD possesses a 3D network structure, high specific surface area, exceptional electronic conductivity and satisfactory capacity for biomolecules by virtue of the perfect unification great peculiarity of the three conjugated material. Thus, the 3D-rGO/Fe_3O_4/HP-β-CD coated glassy carbon electrode (GCE) exhibits a strong catalytic property for the electrooxidation of 5-HT, DA and AA, which can be applied to simultaneously detect of these three molecules by differential pulse voltammetry (DPV) mode. This sensing platform displays high sensitivity, wide linear range and low detection limit in simultaneous determination. Additionally, this electrochemical sensor was also selected to detect real sample with satisfactory recoveries, indicating a great potential of 3D-rGO/Fe_3O_4/HP-β-CD nanocomposite as electrode material in electroanalytical practices.

Experimental section

Materials and instruments

Ammonia solution ($NH_3 \cdot H_2O$, 25%), HP-β-CD, ferric chloride hexahydrate ($FeCl_3 \cdot 6H_2O$), graphite powder, L-cysteine (L-Cys), 1-(3-dimethylaminopropyl)-3-ethylcarbodiimidehydro chloride (EDC·HCl), 4-dimethylaminopyridine (DMAP) were offered by Shanghai Macklin Biochemical Co. Ltd (http://www.macklin.cn/). 5-HT, DA and AA were provided by Aladdin Industrial Corporation from Shanghai (http://www.aladdin-e.com/). The human hepatoblastoma HepG2 Cells were taken from Shanxi Dayi Hospital. The ultrapure water has been supplied by Millipore system. The size and morphology of the nanomaterials were measured by SEM (S-4800, Hitachi, Japan) besides transmission electron microscopy (TEM, Jem-2100F, Jeol). The XRD (Bruker, D8 Advance), FT-IR (Bruker, Tensor), Raman (Horiba 800) and XPS (Thermo Scientific, ESCALAB 250Xi) have also been used to character the structure and elemental composition of nanocomposites. The electrochemical experiments were accomplished using an electrochemical workstation (CHI 660E, Chenhua, China) in the identical system encompassing three-electrode with our previous work [15]. All the details of electrochemical experiment information have been described in Electronic Supporting Material (ESM).

Fabrication of 3D-rGO/Fe_3O_4/HP-β-CD

Firstly, 3D-rGO/Fe_3O_4 (prepared in ESM) was sonicated in ultrapure water for several minutes so that it was completely dispersed. After activation the surface of carboxylic groups from 3D-rGO/Fe_3O_4 using EDC•HCl (46 mg, 0.24 mmol) for 3h, the appropriate amounts of HP-β-CD powder was added into above solution with a combination of DMAP (29 mg, 0.24 mmol) to make ester bonds between the carboxyl groups of 3D-rGO/Fe_3O_4 and hydroxyl groups of HP-β-CD. Then the vial was kept stirring for 24 h at room temperature to give 3D-rGO/Fe_3O_4/HP-β-CD. Finally, the nano-composites were washed with ultrapure water and anhydrous ethanol, collected with the aid of an external magnet repeatedly, and freeze-dried to yield a black powder.

Fabrication of 3D-rGO/Fe_3O_4/HP-β-CD/GCE

After carefully polishing the bare glassy carbon electrode (GCE, 3 mm in diameter) using alumina powder, and washing it with doubly deionized water and ethanol, the electrode was naturally dried. 3D-rGO/Fe_3O_4/HP-β-CD was dispersed in ultrapure water by ultrasonication, and 5 μL of the ~~resulting~~ 3D-rGO/Fe_3O_4/HP-β-CD suspension solution (2 mg·mL^{-1}) was modified onto clean GCE surface, and finally dried by infrared lamp. The 3D-rGO/Fe_3O_4 and 3D-rGO modified GCE were constructed with similar preparation process. The other electrochemical experiment information are presented in ESM.

Real sample analysis

The 3D-rGO/Fe_3O_4/HP-β-CD modified electrode was applied to detect 5-HT, DA and AA from human serum sample (provided by Shanxi Dayi Hospital) to evaluate its reliability for practical applications. Briefly, interfering proteins in pristine serum removed by centrifugation at 8000 rpm. Next, the serum samples were diluted 1:5 and 1:50 with 0.1 M phosphate buffer (PB) (pH = 7.0). 10 mL of diluted serum solution was transferred to the electrochemical cell for DPV analysis using 3D-rGO/Fe_3O_4/HP-β-CD/GCE to obtain the original amount of 5-HT, DA and AA in serum. Further tests were conducted for quantitative analysis with the standard addition method by adding different volumes of the standard solution of 5-HT, DA and AA. Then, the spiked 5-HT, DA and AA were also analyzed by DPV.

Results and discussion

Characterization of the 3D-rGO/Fe_3O_4/HP-β-CD

The surface morphology and size distribution of the 3D-rGO/Fe_3O_4/HP-β-CD were conducted by TEM besides SEM. From the SEM photograph in Fig. 1A, a well-defined polyporous and interconnected 3D framework was shaped by the crosslinked coordination and haphazard orientation of stacked rGO sheets. However, compared with the 3D-rGO/Fe_3O_4 (Fig. S1†), the introduction of HP-β-CD in 3D-rGO/Fe_3O_4/HP-β-CD hybrids failed to influence the 3D structure of our nanocomposite. Clearly, the TEM image (Fig. 1B) shows typical crumpled structure caused by a large amount of 3D-rGO nanosheets with many wrinkles. The dark spots corresponding to Fe_3O_4 nanoparticles seem to be uniformly embedded into the network of 3D-rGO. As can been seen from the HRTEM photograph (Fig. 1C), the thickness of the graphene sheets is

about 3 nm, and the average diameter of the Fe_3O_4 nanoparticle is estimated to be about 8 nm.

Further information is provided for the HP-β-CD successful cross-linked 3D-rGO/Fe_3O_4. FT-IR spectrogram of 3D-rGO/Fe_3O_4/HP-β-CD as well as pristine HP-β-CD, 3D-rGO and 3D-rGO/Fe_3O_4 are depicted in Fig. 2A. For HP-β-CD, the stretching vibration of O-H is exhibited a broad and strong peak at 3400 cm^{-1}, and the peak in position of 1647 cm^{-1} is attributable to C=C stretching vibrations. The significant peaks between 1200 cm^{-1} and 1000 cm^{-1} are considered as the feature of HP-β-CD. Compared to 3D-rGO, the appearance of C=O at 1720 cm^{-1} for 3D-rGO/Fe_3O_4 suggests that the OH groups of Fe_3O_4 reacted with the COOH groups situated at the sides of the 3D-rGO layers. Two featured bands at 1175 cm^{-1} and 1020 cm^{-1} are owed to the epoxy C-O and alkoxy C-O stretching vibrations, respectively. Besides, it also shows the bands due to the stretching vibrations (2927 cm^{-1}, 2971 cm^{-1}) and bending vibration (742 cm^{-1}) of C-H on the phenyl ring. Corresponding to the bare Fe_3O_4, the representative peak of stretching vibration of Fe-O bond at around 533 cm^{-1} indicates that the Fe_3O_4 is successfully bound to the 3D-rGO. Thus, the typical cyclodextrin and Fe_3O_4 absorption features of 3D-rGO/Fe_3O_4/HP-β-CD exhibiting in the FT-IR spectrogram conclude the successful generation of 3D-rGO/Fe_3O_4/HP-β-CD.

Raman spectroscopy is employed to identify the quality and structural characterization of graphene family materials [31]. Fig. 2B exhibits the various Raman spectrogram of GO, 3D-rGO, 3D-rGO/Fe_3O_4 and 3D-rGO/Fe_3O_4/HP-β-CD. For original GO, there exist two distinct bands approximately at 1346 cm^{-1} (D band, for defect or disorder) and 1600 cm^{-1} (G band), respectively. The ratio of D-/G-intensity (I_D/I_G) was expected to quantify the degree of disorder, and it was calculated to be 0.92 for GO. For 3D-rGO curve, I_D/I_G ratio increases on account of the synthesis of 3D framework in the process of reduction of GO resulting in the increasing of carbon cavities and disordered degree. In the case of 3D-rGO/Fe_3O_4, an enhanced I_D/I_G ratio (1.42) confirms the introduction of Fe_3O_4 nanoparticles onto the 3D network. After 3D-rGO/Fe_3O_4 was functionalized with HP-β-CD, it was observed that the I_D/I_G value distinctly decreases (1.01) in comparison with 3D-rGO/Fe_3O_4 as a result of the partial disappearance of defects during chemical functionalization. Additionally, a relatively weaker 2D band (2701 cm^{-1}) and a strong G band (1589 cm^{-1}) obviously lead to $I_G/I_{2D} > 1$, indicating the fact that 3D-rGO/Fe_3O_4/HP-β-CD is multi-layered. Besides, XRD (Fig. S2) and XPS (Fig. S3) results also provide some crucial evidences for the successful

synthesis of 3D-rGO/Fe_3O_4/HP-β-CD. And biocompatibility patterns were performed and illustrated the nontoxicity of 3D-rGO/Fe_3O_4/HP-β-CD under the tested concentration conditions (Fig. S4).

Electrochemical measurement of the sensor fabrication

EIS was employed to determine the electrochemical characteristics during preparation process, shown in Fig. 3A. A Randles equivalent circuit was applied to fit the EIS data. As depicted in the inset of Fig. 3A, the circuit includes the electrolyte resistance between the working and reference electrodes (R_s), the double layer capacitance of electrode and electrolyte (C), Warburg impedance (Z_w), and electron transfer resistance (R_{ct}) by the diffusion of ions from the electrolyte to the interface. The EIS value R_{et} of bare GCE is the largest (320 Ω, RSD: 2.3%), illustrating that the electron transfer of bare GCE is the most difficult one among the four nanomaterials. As to 3D-rGO/Fe_3O_4/GCE, its semicircle diameter is significantly smaller compared to the value of 3D-rGO/GCE, and the R_{ct} of 68 Ω (RSD: 2.5%) was indeed less than that of 3D-rGO/GCE (166 Ω, RSD: 3.2%). This may result from the synergy linking of Fe_3O_4 and 3D-rGO that makes the interfacial electron transfer easy for 3D-rGO/Fe_3O_4/GCE. When GCE was modified by 3D-rGO/Fe_3O_4/HP-β-CD, the lowest R_{ct} (15 Ω, RSD: 4.6%) value is obtained among all the modified electrodes, indicating that the grafting of HP-β-CD contributes to enhancing the transfer rate of 3D-rGO/Fe_3O_4/HP-β-CD nanohybrids.

Additionally, the effective surface areas (A) of 3D-rGO/Fe_3O_4/HP-β-CD/GCE and bare GCE were also explored by chronocoulometry in 0.1 mM $K_3[Fe(CN)_6]$ containing 1.0 M KCl (diffusion coefficient, $D = 7.6\times10^{-6}$ $cm^2\cdot s^{-1}$, at 25 °C [32]). The corresponding values of A were calculated to be 0.7439 and 0.1758 cm^2, respectively, which obviously proves the effective area of the 3D-rGO/Fe_3O_4/HP-β-CD/GCE is approximately 4-fold high as much as that of the bare GCE. This further demonstrates that 3D-rGO/Fe_3O_4/HP-β-CD modified GCE can improve greatly surface area of the electrode (Fig. S5).

3D-rGO/Fe_3O_4/HP-β-CD/GCE for electrochemical detection of 5-HT, DA and AA

The possibility of simultaneous detection of 5-HT, DA and AA has been investigated by

using 3D-rGO/Fe_3O_4/HP-β-CD/GCE. Fig. 3B displays DPVs of bare GCE, 3D-rGO/GCE, 3D-rGO/Fe_3O_4/GCE and 3D-rGO/Fe_3O_4/HP-β-CD/GCE in 0.1 M PB, in which 10 μM 5-HT, 40 μM DA and 400 μM AA co-existed. Only a rather broad oxidation peak appeared at bare GCE, which leads to peak potentials for these three analytes using bare GCE are indistinguishable, further revealing the poor selectivity towards these three biomolecules. It is very apparent that the distinctly distinguishable peaks at 0.316, 0.16 and -0.044 V using 3D-rGO/Fe_3O_4/HP-β-CD/GCE corresponds to the respectively electrochemistry oxidation of 5-HT, DA and AA. The difference in anode peak potential between 5-HT and DA, DA and AA, 5-HT and AA are 0.156 V, 0.204 V and 0.36 V, respectively, which ensure the simultaneous detection of these three biomolecules by 3D-rGO/Fe_3O_4/HP-β-CD/GCE. In fact, the well-defined anodic peaks for three targets can also be given by 3D-rGO/Fe_3O_4/GCE and 3D-rGO/GCE, but the oxidation current for three molecules are much lower than those at 3D-rGO/Fe_3O_4/HP-β-CD/GCE. The increased current response at 3D-rGO/Fe_3O_4/HP-β-CD/GCE might be ascribed to the fact that HP-β-CD can give a unique host-guest interaction for the detected biomolecules, which evidently boost the electrochemical sensitivity and selectivity of electrode. Considering that 3D-rGO/Fe_3O_4/HP-β-CD/GCE displays the highest current response in terms of DPVs (Fig. 3B) and CVs (Fig. S6), the 3D-rGO/Fe_3O_4/HP-β-CD/GCE was applied to independent and simultaneous detection of 5-HT, DA and AA in the follow-up measurements via DPV mode. In addition, the exploration of the oxidation mechanism for analytes was performed, as shown in Fig. S7 and Fig. S8.

Optimization of determination conditions

To achieve the better sensing behavior for simultaneous determination of 5-HT, DA and AA, the following parameters were optimized in the experiment: (a) pH value of PB; (b) accumulation time; (c) volume of 3D-rGO/Fe_3O_4/HP-β-CD dispersion. Respective data and figures are provided in the ESM (Fig. S9-S12). Experimental determination conditions were found to give best results: (a) Optimal pH of PB: 7.0; (b) Optimal accumulation time: 6 min; (c) Optimal amount of the modifier: 5 μL.

Electrochemical quantification of 5-HT, DA, AA

Furthermore, under the optimum experimental conditions mentioned above, the individual

and simultaneous quantitative determination of 5-HT, DA or AA was implemented respectively. Fig. 4 presents DPVs results of independent 5-HT (A), DA (B), AA (C) and three molecules mixed solution (D) achieved at according various concentrations by 3D-rGO/Fe_3O_4/HP-β-CD/GCE. And Fig. S13 displays the calibration plots corresponding to Fig. 4. A significant observation was made in terms of three analytes that the great linearity was obtained in various concentration ranges with the detection limits whether individual or simultaneous quantitative detection of 5-HT, DA and AA. All the quantitative analysis results of individual and simultaneous detection have been described in Table 1.

Noticeably, the similar slope of linear analytical curve for each molecule was acquired in the simultaneous and individual tests, which indicates that the 5-HT, DA and AA do not interfere each other in the simultaneous quantitative determination at 3D-rGO/Fe_3O_4/HP-β-CD/GCE. Table 2 shows that, in contrast to other sensors [8, 11, 12, 22, 23, 33-40], the 3D-rGO/Fe_3O_4/HP-β-CD-modified GCE shows superior distinguishability and high sensitivity.

Repeatability and stability and practical sample analysis

Repeatability of 3D-rGO/Fe_3O_4/HP-β-CD/GCE was estimated from the DPV response to simultaneously detecting of 20 μM 5-HT, 10 μM DA and 300 μM AA by parallel four measurements with the same electrode (Fig. S14). The relative standard deviations (RSD) of 5-HT, DA and AA have been calculated to be 3.9%, 2.6%, 3.2%, displaying satisfactory repeatability of the modified electrode. In addition, after the 3D-rGO/Fe_3O_4/HP-β-CD/GCE was kept in PB (0.1 M, pH 7) under 4 °C about 1 month, no obvious current response decay has been perceived (Fig. S15), exhibiting the good stability of the 3D-rGO/Fe_3O_4/HP-β-CD/GCE. To investigate the practicability of the 3D-rGO/Fe_3O_4/HP-β-CD/GCE, simultaneously detecting of 5-HT, DA and AA has been performed in human serum sample using 3D-rGO/Fe_3O_4/HP-β-CD/GCE with the standard addition method. The mixed samples containing various concentrations of three small biomoleculesare gradually added to the serum for the DPV recording. The quantitative results (Table S1) are calculated by the DPV detection of 5-HT, DA and AA in varied diluted serum samples by 3D-rGO/Fe_3O_4/HP-β-CD/GCE. Under the detected conditions, the concentrations of 5-HT and AA are respectively found to be 0.75 and 59.5 μM, whereas DA fails to be found in the pristine serum sample. The acceptable recoveries of

96.9%-103% were obtained for 5-HT, 97.3%-102% for DA and 96.3%-105% for AA, which confirm that the 3D-rGO/Fe_3O_4/HP-β-CD/GCE is credible for the practical sample detections.

Summary

A sensitive assay has been constructed by using 3D-rGO/Fe_3O_4/HP-β-CD modified GCE, and successfully applied to simultaneously detect of 5-HT, DA and AA. The 3D-rGO/Fe_3O_4 has a specific 3D-network structure, high conductivity and efficient catalytic activity, while HP-β-CD exhibits host-guest interactions with small biomolecules. Based on these unique characteristics, the 3D-rGO/Fe_3O_4/HP-β-CD biosensor provides enhanced peak current responses towards single 5-HT, DA and AA solution with wide linear ranges and limits of detection as low as 6.7 nM, 3.3 nM and 5 μM, however, the corresponding value are 3.3 nM, 6.7 nM and 3.3 μM for ternary mixture, respectively. Further application for the detections of 5-HT, DA and AA in serum samples was also demonstrated with satisfactory results. Thus, we anticipate that the present development has laid the foundation of potential application of the 3D graphene nanohybrid-based electrochemical biosensor in clinical detection and medical testing.

Acknowledgements

This work was conducted with the support of the National Natural Science Foundation of China (No. 21976113, 21871194, 21707082, 21874087, and 21575084), the Natural Science Foundation of Shanxi Province (No. 201801D221059, 201801D121040), the Hundred Talent Program of Shanxi Province, the Hong Kong Research Grants Council (PolyU 153051/17P) and the Hong Kong Polytechnic University (1-ZE1C and 847S). We are especially grateful for Scientific Instrument Center of Shanxi University providing XRD analysis.

References

[1] Nichols DE, Nichols CD (2008) Serotonin receptors. Chem Rev 108: 1614-1641.

[2] Arrigoni O, Tullio CD (2002) Ascorbic acid: much more than just an antioxidant. Biochim Biophys Acta 1569: 1-9.

[3] Nieoullon A, Coquerel A (2003) Dopamine: a key regulator to adapt action, emotion, motivation and cognition. Curr Opin Neurol 16: S3-S9.

[4] Wightman RM, May LJ, Michae AC (1988) Detection of dopamine dynamics in the brain. Anal Chem 60: 769A-779A.

[5] Mo JW, Ogorevc B (2001) Simultaneous measurement of dopamine and ascorbate at their physiological levels using voltammetric microprobe based on overoxidized poly(1,2-phenylenediamine)-coated carbon fiber. Anal Chem 73: 1196-1202.

[6] Wang Y, Xia YS (2019) Optical, electrochemical and catalytic methods for in-vitro diagnosis using carbonaceous nanoparticles: a review. Microchim Acta 186: 50.

[7] Batool R, Akhtar MA, Hayat A, Han DX, Niu L, Ahmad MA, Nawaz MH (2019) A nanocomposite prepared from magnetite nanoparticles, polyaniline and carboxy-modified graphene oxide for non-enzymatic sensing of glucose. Microchim Acta 186: 267.

[8] Li SM, Wang YS, Hsiao ST, Liao WH, Lin CW, Yang SY, Tien HW, Ma CCM, Hu CC (2015) Fabrication of a silver nanowire-reduced graphene oxide-based electrochemical biosensor and its enhanced sensitivity in the simultaneous determination of ascorbic acid, dopamine, and uric acid. J Mater Chem C 3: 9444-9453.

[9] Khohnevisan K, Maleki H, Honarvarfard E, Baharifar H, Gholami M, Faridbod F, Larijani B, Majidi RF, Khorramizadeh MR (2019) Nanomaterial based electrochemical sensing of the biomarker serotonin: a comprehensive review. Microchim Acta 186: 49.

[10] Wei J, He JB, Cao SQ, Zhu YW, Wang Y, Hang GP (2010) Enhanced sensing of ascorbic acid, dopamine and serotonin at solid carbon paste electrode with a nonionic polymer film. Talanta 83: 190-196.

[11] Jin GP, Lin XQ, Gong JM (2004) Novel choline and acetylcholine modified glassy carbon electrodes for simultaneous determination of dopamine, serotonin and ascorbic acid. J Electroanal Chem 569: 135-142.

[12] Zhou JQ, Sheng ML, Jiang XY, Wu GZ, Gao F (2013) Simultaneous determination of dopamine, serotonin and ascorbic Acid at a glassy carbon electrode modified with carbon-spheres. Sensors 13: 14029-14040.

[13] Li C, Shi G (2012) Three-dimensional graphene architectures. Nanoscale 4: 5549-5563.

[14] Lu LP, Guo LQ, Kang TF, Cheng SY (2017) A gold electrode modified with a three-dimensional graphene-DNA composite for sensitive voltammetric determination of dopamine. Microchim Acta 184: 2949-2957.

[15] Liang WT, Rong YQ, Fan LF, Dong WJ, Dong QC, Yang C, Zhong ZH, Dong C, Shuang SM, Wong WY (2018) 3D graphene/hydroxypropyl-β-cyclodextrin nanocomposite as an electrochemical chiral sensor for the recognition of tryptophan enantiomers. J Mater Chem C 6: 12822-12829.

[16] Zhang Y, Huang BT, Yu F, Yuan QH, Gu M, Ji JY, Zhang Y, Li YC (2018) 3D nitrogen-doped graphite foam@Prussian blue: an electrochemical sensing platform for highly sensitive determination of H_2O_2 and glucose. Microchim Acta 185: 86.

[17] Zhao YN, Zhou J, Jia ZM, Huo DQ, Liu QY, Zhong DQ, Hu Y, Yang M, Bian MH, Hou, CJ (2019). In-situ growth of gold nanoparticles on a 3D-network consisting of a MoS_2/rGO nanocomposite for simultaneous voltammetric determination of ascorbic acid, dopamine and uric acid. Microchim Acta 186: 92.

[18] Esmaeilpour M, Sardarian AR, Javidi J (2012) Schiff base complex of metal ions supported on superparamagnetic Fe_3O_4@SiO_2 nanoparticles: An efficient, selective and recyclable catalyst for synthesis of 1,1-diacetates from aldehydes under solvent-free conditions. Appl Catal A-Gen 445: 359-367.

[19] Kumar R, Singh RK, Vaz AR, Savu RSA, Moshkalev SA (2017) Self-assembled and one-step synthesis of interconnected 3D network of Fe_3O_4/reduced graphene oxide nanosheets hybrid for high-performance supercapacitor electrode. ACS Appl Mater Inter 9: 8880-8890.

[20] Wang QQ, Zhang XP, Huang L, Zhang ZQ, Dong SJ (2017) One-pot synthesis of Fe_3O_4 nanoparticle loaded 3D porous graphene nanocomposites with enhanced nanozyme activity for glucose detection. ACS Appl Mater Inter 9: 7465-7471.

[21] Qiu N, Liu Y, Xiang M, Lu XM, Yang Q, Guo R (2018) A facile and stable colorimetric sensor based on three-dimensional graphene/mesoporous Fe_3O_4 nanohybrid for highly sensitive and selective detection of p-nitrophenol. Sensors Actuators B chem 266: 86-94.

[22] Chang Z, Zhou YL, Hao LJ, Hao YQ, Zhu X, Xu MT (2017) Simultaneous determination of dopamine and ascorbic acid using β-cyclodextrin/Au nanoparticles/graphene-modified electrodes. Anal Methods 9: 664-671.

[23] Abbaspour A, Noori A (2011) A cyclodextrin host–guest recognition approach to an electrochemical sensor for simultaneous quantification of serotonin and dopamine. Biosens Bioelectron 26: 4674-4680.

[24] Niu XH, Mo ZL, Yang X, Sun MY, Zhao P, Li ZL, Ouyang MX, Liu ZY, Gao HH, Guo RB, Liu NJ (2018) Advances in the use of functional composites of β-cyclodextrin in electrochemical sensors. Microchim Acta 185: 328.

[25] Feng WL, Liu C, Lu SY, Zhang CY, Zhu XH, Liang Y, Nan.JM (2014) Electrochemical chiral recognition of tryptophan using a glassy carbon electrode modified with β-cyclodextrin and graphene. Microchim Acta 181: 501-509.

[26] Upadhyay SS, Kalambate PK, Srivastava AK (2017) Enantioselective analysis of moxifloxacin hydrochloride enantiomers with graphene-β-cyclodextrin-nanocomposite modified carbon paste electrode using adsorptive stripping differential pulse Voltammetry. Electrochim Acta 248: 258-269.

[27] Liang WT, Yang C, Zhou DY, Haneoka H, Nishijima M, Fukuhara G, Mori T, Castiglione F, Mele A, Caldera F, Trotta F, Inoue Y (2013) Phase-controlled supramolecular photochirogenesis in cyclodextrin nanosponges. Chem Commun 49: 3510-3512.

[28] Liang WT, Huang Y, Lu DT, Ma XW, Gong T, Cui XD, Yu BF, Yang C, Dong C, Shuang SM (2019) β-Cyclodextrin-hyaluronic acid polymer functionalized magnetic graphene oxide nanocomposites for targeted photo-chemotherapy of tumor cells. Polymers 11: 133.

[29] Chaudhuri S, Chakraborty S, Sengupta PK (2010) Encapsulation of serotonin in β-cyclodextrin nano-cavities: Fluorescence spectroscopic and molecular modeling studies. J Mol Struct 975: 160-165.

[30] Palomar-Pardavé M, Alarcón-ángeles G, Ramírez-Silva MT, Romero-Romo M, Rojas-Hernández A, Corona-Avendano S (2011) Electrochemical and spectrophotometric determination of the formation constants of the ascorbic acid-β-cyclodextrin and dopamine-β-cyclodextrin inclusion complexes. J Incl Phenom Macrocycl Chem 69: 91-99.

[31] Dresselhaus MS, Jorio A, Souza Filho AG, Saito R (2010) Defect characterization in graphene and carbon nanotubes using Raman spectroscopy. Phil Trans R Soc A 368: 5355-5377.

[32] Adams RN (1969) Electrochemistry at solid electrodes. Marcel Dekker, New York, 1969.

[33] Torabi R, Compton RG (2007) A simple electroanalytical methodology for the simultaneous determination of dopamine, serotonin and ascorbic acid using an unmodified edge plane pyrolytic graphite electrode. Anal Bioanal Chem 387: 2793-2800.

[34] Khan Md. ZH, Liu XQ, Tang YF, Zhu JH, Hu WP, Liu XH (2018) A glassy carbon electrode modified with a composite consisting of gold nanoparticle, reduced graphene oxide and poly(L-arginine) for simultaneous voltammetric determination of dopamine, serotonin and L-tryptophan. Microchim Acta 185: 439.

[35] Jiang XH, Lin XQ (2005) Overoxidized polypyrrole film directed DNA immobilization for construction of electrochemical micro-biosensors and simultaneous determination of serotonin and dopamine. Anal Chim Acta 537: 145-151.

[36] Han HS, Lee HK, You JM, Jeong H, Jeon S (2014) Electrochemical biosensor for simultaneous determination of dopamine and serotonin based on electrochemically reduced-GO-porphyrin. Sensors Actuators B chem 190: 886-895.

[37] Sun DF, Li HJ, Li MJ, Li CP, Dai HL, Sun DZ, Yang BH (2018) Electrodeposition synthesis of a NiO/CNT/PEDOT composite for simultaneous detection of dopamine, serotonin, and tryptophan. Sensors Actuators B chem 259: 433-442.

[38] Wang ZH, Liang QL, Wang YM, Luo GA (2003) Carbon nanotube-intercalated graphite electrodes for simultaneous determination of dopamine and serotonin in the presence of ascorbic acid. J Electroanal Chem 540: 129-134.

[39] Deng WF, Yuan XY, Tan YM, Ma M, Xie QJ (2016) Three-dimensional graphene-like carbon frameworks as a new electrode material for electrochemical determination of small biomolecules. Biosens Bioelectron 85: 618-624.

[40] Huang HP, Yue YF, Chen ZZ, Chen YN, Wu SZ, Liao JS, Liu SJ, Wen HR (2019) Electrochemical sensor based on a nanocomposite prepared from $TmPO_4$ and graphene oxide for simultaneous voltammetric detection of ascorbic acid, dopamine and uric acid. Microchim Acta, 186: 189.

.

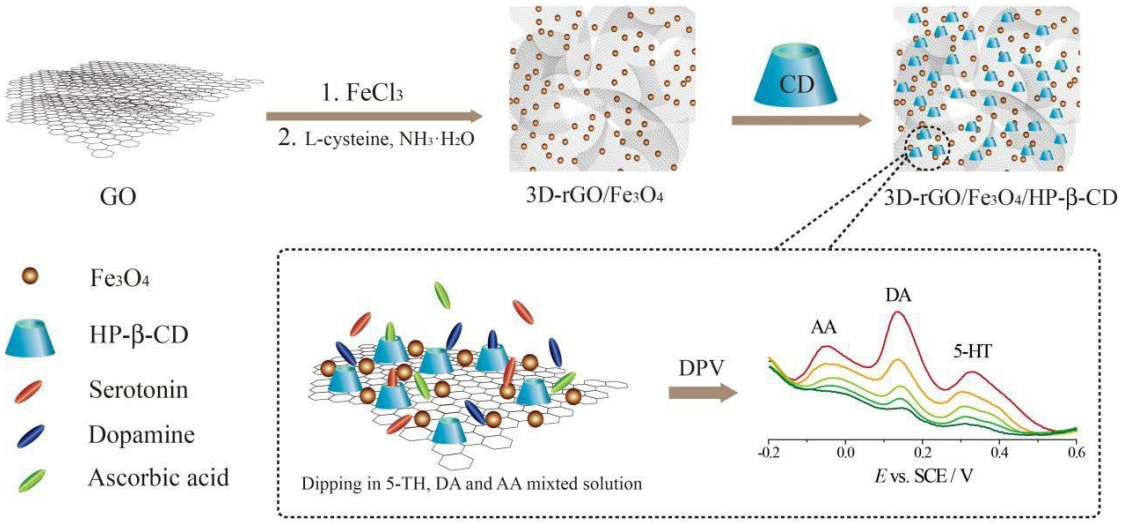

Scheme 1. Schematic diagram for constructing 3D-rGO/Fe_3O_4/HP-β-CD, and simultaneous detecting serotonin (5-HT), dopamine (DA) and ascorbic acid (AA) by an electrochemical strategy.

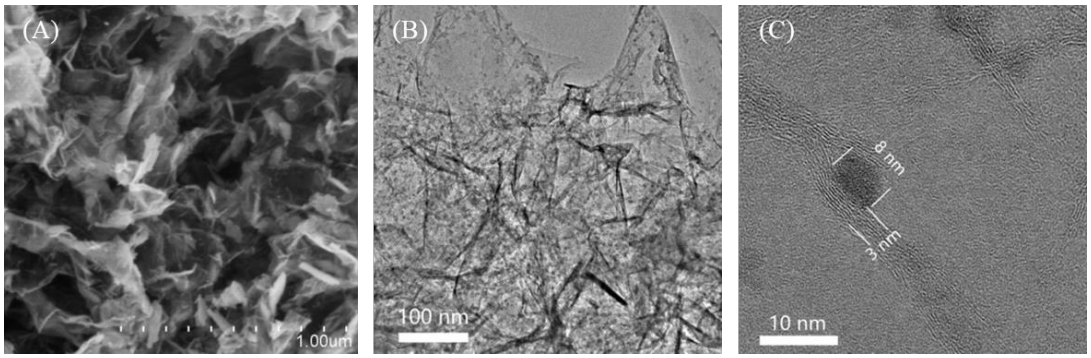

Fig. 1. SEM (A), TEM (B) and HRTEM(C) photographs of 3D-rGO/Fe_3O_4/HP-β-CD

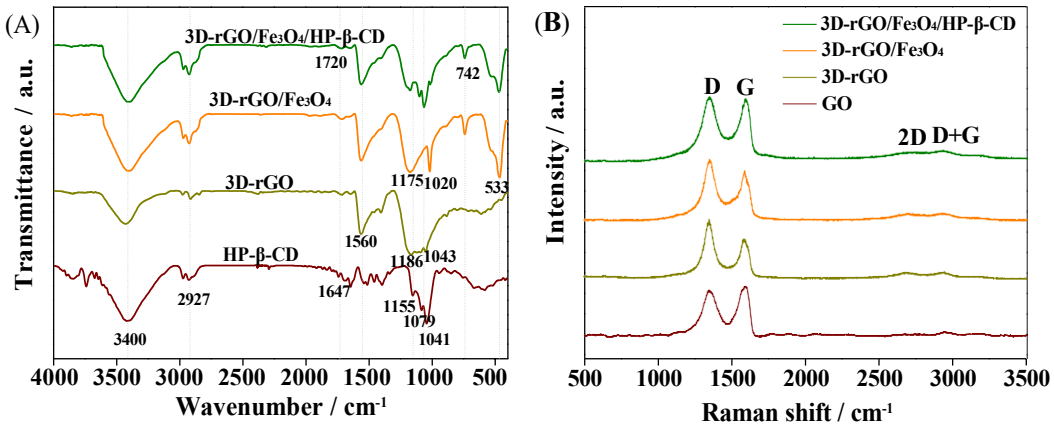

Fig. 2. (A) FT-IR spectrogram of HP-β-CD, 3D-rGO, 3D-rGO/Fe_3O_4 and 3D-rGO/Fe_3O_4/HP-β-CD; (B) XRD analysis of the 3D-rGO/Fe_3O_4 and 3D-rGO/Fe_3O_4/HP-β-CD.

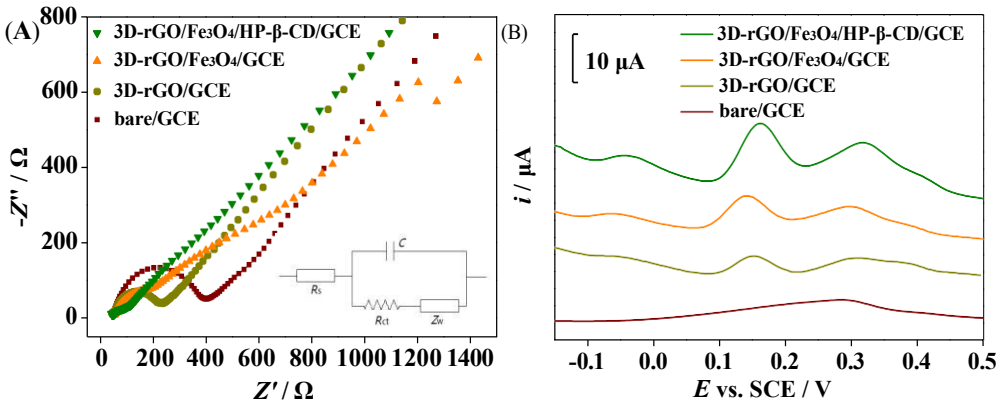

Fig. 3. (A) Nyquist plots of bare GCE, 3D-rGO, 3D-rGO/Fe_3O_4 and 3D-rGO/Fe_3O_4/HP-β-CD modified GCE in a 10.0 mL 0.1 M PB containing 5 mM $[Fe(CN)_6]^{3-/4-}$ and 0.1 M KCl (pH 7.0) (Amplitude: 0.005 V, potential: 0.188 V, frequency range:10 mHz - 100 kHz.). (B) DPVs of 3D-rGO/Fe_3O_4/HP-β-CD/GCE, 3D-rGO/Fe_3O_4/GCE, 3D-rGO and bare GCE in 0.1 M PB of pH 7.0 containing 10 μM 5-HT, 40 μM DA, and 400 μM AA. (Amplitude: 0.05 V, increment potential: 0.004 V, pulse width: 0.05 s, pulse period: 0.5 s, quiet time: 2 s.)

.

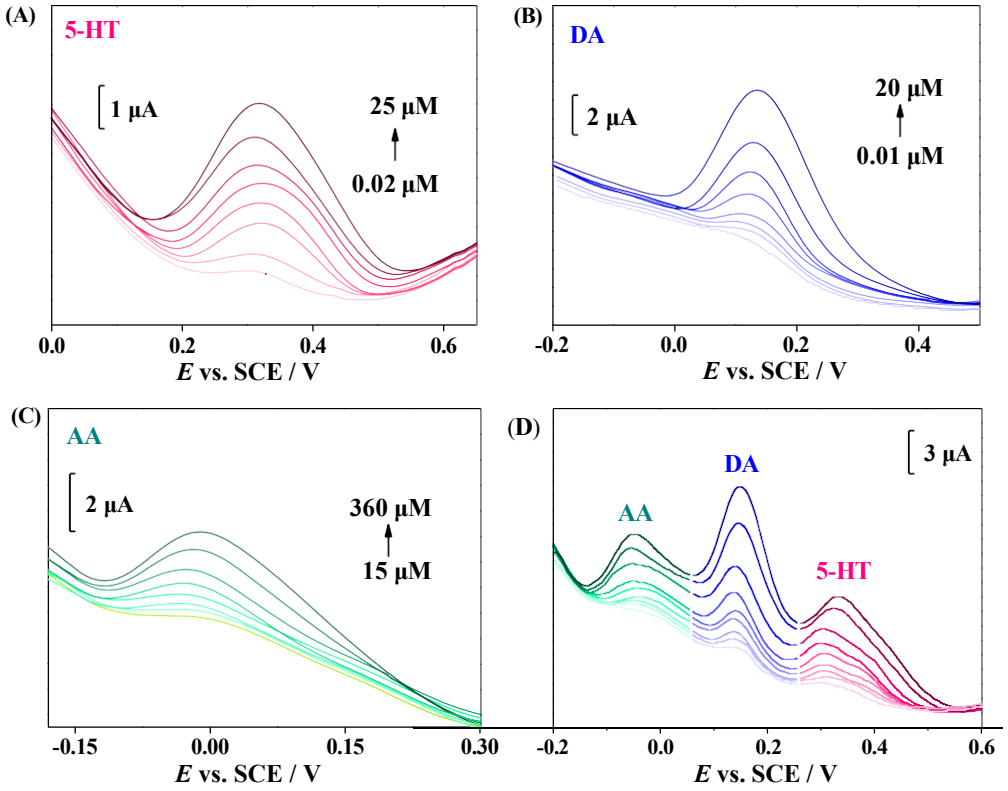

Fig. 4. Individual quantitative detection of 5-HT (A) or DA (B) or AA (C) and simultaneously quantitative detection of 5-HT, DA and AA (D) by 3D-rGO/Fe_3O_4/HP-β-CD/GCE in 0.1 M PB of pH 7.0. (Amplitude: 0.05 V, increment potential: 0.004 V, pulse width: 0.05 s, pulse period: 0.5 s, quiet time: 2 s.)

Table 1. Determination data analysis of individual and simultaneous detection of 5-HT, DA and AA.

Detection way	Analytes	Linear calibration curves (linear correlation coefficient)	Linearity range/μM	Detection limits (S/N=3)
Individual quantitative detection	5-HT	i (μA)=0.33+0.11c (μM) (R^2=0.9995)	0.02-25	6.7 nM
	DA	i (μA)=0.20+0.39c (μM) (R^2=0.9985)	0.01-20	3.3 nM
	AA	i (μA)=0.22+0.01c (μM) (R^2=0.9990)	15-360	5 μM
Simultaneous quantitative detection	5-HT	i (μA)=0.35+0.12c (μM) (R^2=0.9987)	0.01-25	3.3 nM
	DA	i (μA)=0.23+0.35c (μM) (R^2=0.9984)	0.02-25	6.7 nM
	AA	i (μA)=0.20+0.011c (μM) (R^2=0.9988)	10-350	3.3 μM

Table 2. Comparison of analytical performance over various modified electrodes

Electrode	Linear range (μM)			Detection limit (μM)			Detection way	Ref.
	5-HT	DA	AA	5-HT	DA	AA		
EPPGE	0.1-100	0.2-25	0.5-60	0.06	0.09	0.2	simultaneous	33
ACh/GCE	1-30	0.7-5	7-90	0.5	0.3	0.9	simultaneous	11
CS/GCE	40-750	20-150	300-2000	0.7	2	0.6	simultaneous	12
GCE/P-Arg/ErGO/	0.01-0.5	0.001-0.05	—	0.03	0.001	—	individual	34
AuNP	1.0-10	1.0-50						
DNA-PPyox/CFE	0.01-1	0.3-10	—	0.007	0.05	—	individual	35
ERGO-P/GCE	0.1-300	0.1-500	—	0.0049	0.035	—	individual	36
NiO/CNT/PEDOT/	0.3-35	0.03-20	—	0.063	0.026	—	simultaneous	37
GCE								
MWNT-IE	1-15	0.5-10	—	0.2	0.1	—	simultaneous	38
CD/PNAANI/CNT	4-200	4-200	—	<1	<1	—	simultaneous	23
/CPE								
3DGLCFs/GCE	—	0.05-10	12.5-400	—	0.01	2	individual	39
β-CD/AuNPs/EDG	—	0.5-120	50-900	—	0.024	2.0	simultaneous	22
O/GCE								
GO/$TmPO_4$/GCE	—	2-20	100-1000	—	0.785	39.0	simultaneous	40
AgNW–rGO/SPCE	—	40-450	45-1550	—	0.26	0.81	simultaneous	8
3D-rGO/Fe_3O_4/HP-	0.02-25	0.01-20	15-360	0.0067	0.0033	5	individual	This
β-CD/GCE	0.01-25	0.02-25	10-350	0.0033	0.067	3.3	simultaneous	work

Graphical abstract

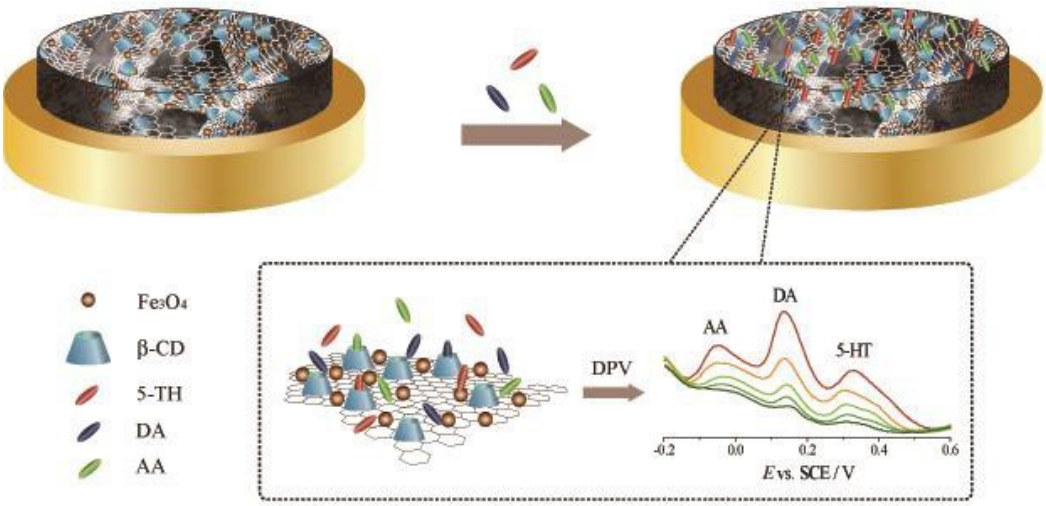

Schematic presentation of simultaneous detecting serotonin (5-HT), dopamine (DA) and ascorbic acid (AA) for three-dimensional reduced-graphene oxide/Fe_3O_4/hydroxypropyl-β-cyclodextrin (3D-rGO/Fe_3O_4/HP-β-CD) by differential pulse voltammetry (DPV) approach.